JOURNAL OF MATERIALS SCIENCE 33 (1998) 2385–2390

# Stability of metastable phases and microstructures in the ageing process of Al–Mg–Si ternary alloys

M. TAKEDA, F. OHKUBO*, T. SHIRAI
*Department of Mechanical Engineering and Materials Science, Yokohama National University, Tokiwadai 79-5 Hodogayaku Yokohama 240, Japan*
*E-mail: t1k4d1@post.post.mc.ynu.ac.jp*

K. FUKUI
*Research Centre, Oyama Factory, Showa Aluminium Co., Inuzuka 480, Oyama, Tochigi 323, Japan*

Precipitation behaviour of Al–Mg–Si alloys, with balanced (Mg/Si = 2), excess silicon (Mg/Si < 2) and excess magnesium (Mg/Si > 2) compositions, were studied by differential scanning calorimetry (DSC), transmission electron microscopy (TEM), and Vickers hardness tests. Four significant exothermic peaks were observed in DSC curves which were attributed to metastable clusters, β″, β′ and stable β phases. The peaks corresponding to β″ and β′ were formed closely in the DSC curves but showed different behaviour in isothermal annealing. The additional peak verifying the precipitation of phases, which has recently been proposed by some workers, was not detected. Transmission electron microscope observations and Vickers microhardness tests showed that β″ precipitates played a major role in improving the hardness, but not β′ precipitates. 

## 1. Introduction

Aluminium-based Al–Mg–Si ternary alloys are most widely used in applications. Extensive studies of the precipitation behaviour of Al–Mg–Si alloys have been carried out because of the need for fundamental understanding and for practical purposes. The precipitation behaviour of Al–Mg–Si alloys has been generally considered to follow the scheme: supersaturated solid solution (SSSS) → cluster → metastable β″ → metastable β′ → stable β [1–4]. Some papers have claimed the formation of other metastable phases during isothermal heat treatment [5–7]. However, significant ambiguities of the structures, the alloy compositions and the properties of metastable phases still remain.

The precipitation behaviour of Al–Mg–Si alloys is basically investigated based on both the thermal stabilities and the structural aspects of stable/metastable phases. Differential scanning calorimetry (DSC) measurements and transmission electron microscopy (TEM) observations are very helpful tools for this purpose, but there are few works which systematically examine the relation between macroscopic properties, such as thermal stabilities of phases detected by DSC measurements, and the microstructures observed by TEM.

This work aimed to clarify the relation between the precipitation behaviour of Al–Mg–Si alloys during isothermal heat treatment, the phase stability of DSC measurements, and the microstructure observed by TEM.

## 2. Experimental procedure

Three alloy specimens were prepared having the solute composition Mg/Si = 2/1 in atomic ratio, four specimens with excess silicon and four specimens with excess magnesium contents. In this paper we present the experimental results of three balanced alloys, three excess silicon and three excess magnesium alloys which are listed in Table I. The alloys labelled B1–B3 are pseudo-binary Al–$Mg_2Si$ alloys comprising aluminium and solute elements magnesium and silicon, with balanced compositions (Mg/Si = 2/1). The alloys S1–S3 and M1–M3 are those with excess silicon (Mg/Si < 2) and with excess magnesium (Mg/Si > 2) compositions, respectively. The billets, 75 mm in diameter, were extruded at 500 °C. The sheets, 1 mm thick, were obtained by cold-rolling. The final test specimens were solution treated at 555 °C for 60 min and quenched in water at 0 °C. The specimens were aged in an oil-bath at 180, 210 and 240 °C or in an air furnace at 300 and 420 °C.

The DSC measurements were carried out with Rigaku TAS300-8230D in a nitrogen atmosphere at 2, 5, 10 and 20 °C $min^{-1}$. The measurements were performed from room temperature to 600 °C using a high-purity aluminium sample as reference. A Jeol JEM100CX type TEM was operated at 100 kV to observe the microstructures of the alloy specimens after individual heat treatments were given. The bright-field TEM images were taken with the symmetric condition along Al(0 0 1) axes at regions of around

*Present address*: Fibre Optics Division, Sumitomo Electric Ind., 1 Tayacho Sakaeku, Yokohama 244, Japan.

TABLE I Sample specimen (at %)

| | Mg | Si | $Mg_2Si$ | Excess Si | Excess Mg |
|---|---|---|---|---|---|
| B1 | 1.28 | 0.56 | 1.68 | – | 0.16 |
| B2 | 0.83 | 0.40 | 1.19 | – | 0.04 |
| B3 | 0.54 | 0.26 | 0.77 | – | 0.02 |
| S1 | 0.83 | 0.58 | 1.24 | 0.17 | – |
| S2 | 0.83 | 0.71 | 1.25 | 0.29 | – |
| S3 | 0.83 | 0.95 | 1.25 | 0.54 | – |
| M1 | 1.01 | 0.40 | 1.21 | – | 0.20 |
| M2 | 1.18 | 0.37 | 1.12 | – | 0.44 |
| M3 | 1.41 | 0.40 | 1.19 | – | 0.61 |

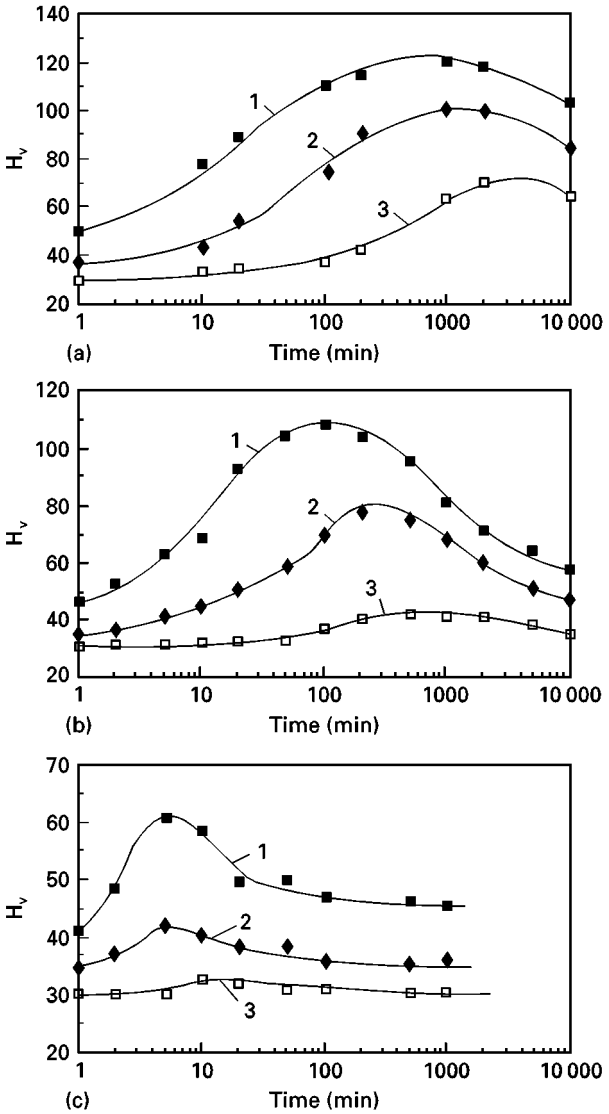


*Figure 1* Changes in Vickers microhardness during isothermal ageing treatments at (a) 180 °C, (b) 210 °C and (c) 240 °C. (1) B1, (2) B2, (3) B3.

20 nm foil thickness, to compare the distributions of precipitates with different TEM specimens. Vickers microhardness tests were conducted using a Shimazu HMV2000 tester.

## 3. Results and discussion

### 3.1. Vickers microhardness of Al–Mg–Si alloys

Fig. 1 shows the Vickers microhardness curves for the alloys B1–B3 obtained by isothermal ageing at 180, 210 and 240 °C. The alloys with higher solute compositions show higher hardness values with no crossing point until 10 000 min. At 210 °C, the hardness curves of the alloys B1–B3 reach the peak position for 100, 200 and 500 min, respectively. Alloy B3 hardly shows a peak at 210 and 240 °C, whereas an increase in hardness occurred at 180 °C. Some previous works mention that Al–Mg–Si alloys with higher solute concentration and those with lower concentration showed different precipitation behaviour in two-step ageing [8–10]. The difference in the present $H_v$ curves suggests that some relation exists between the Vickers hardness curves and the behaviour in two-step ageing, because the difference criteria are both 0.8–0.9 at % $Mg_2Si$ at 210 °C.

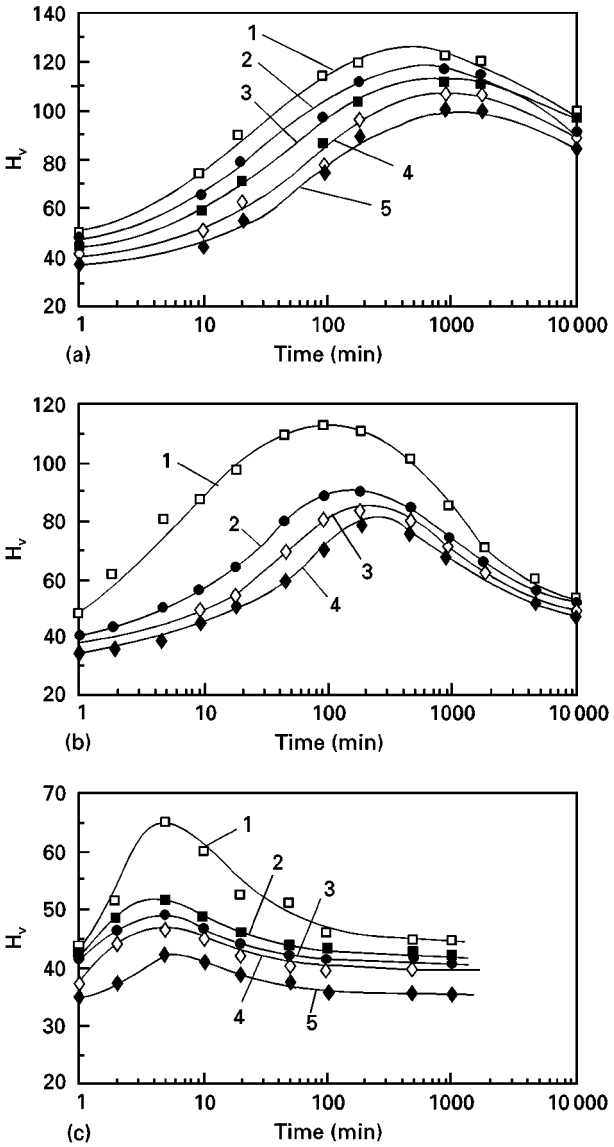


*Figure 2* Changes in Vickers microhardness during isothermal ageing treatments at (a) 180 °C, (b) 210 °C and (c) 240 °C. (a) (1) S2, (2) S1, (3) M2, (4) M1, (5) B2. (b) (1) S3, (2) S1, (3) M1, (4) B2. (c) (1) S3, (2) M3, (3) S1, (4) M1, (5) B2.

Fig. 2 shows the Vickers microhardness curves of excess Si/Mg alloys at 180, 210 and 240 °C, with the reference of B2 alloy. The Al–Mg–Si alloys with excess silicon attain $H_v$ values higher than those of the balanced alloy B2. The presence of magnesium in excess also raises the $H_v$ curves at 180 °C. At higher ageing

temperature, the peaks were shifted towards the initial stage and the enhancement of hardness was lessened in all specimens. The reason why both S1, S2 and M1, M2 alloys showed higher $H_v$ values than the balanced alloy is not clear, but it is obvious that silicon addition is more effective than magnesium in excess, in improving the peak hardness. A possible interpretation will be discussed in the following section.

## 3.2. Thermal stabilities of metastable precipitates

Fig. 3 shows the DSC curves obtained for the alloys B1–B3 starting from the solution-treated condition.

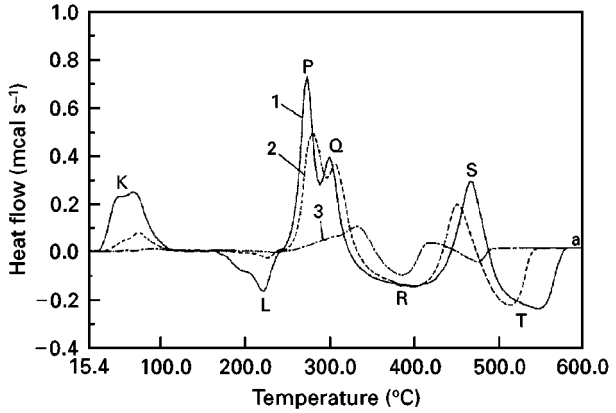


*Figure 3* DSC curves of Al–Mg–Si solution-treated alloys: (1) B1, (2) B2, (3) B3.

The DSC curves of the alloys B1 and B2 have four large exothermic peaks, which appear at around 60 °C (peak K), 270 °C (peak P), 310 °C (peak Q) and 450 °C (peak S). In the DSC curve of the alloy B3, peaks K and P almost disappear. The DSC thermograms support the anticipation that the ageing process of alloy B3 is essentially different from those of B1 and B2. If we relate those exothermic peaks to solute-clusters (β″, β′ and β in the terminology mentioned above), the clustering of solute atoms or precipitation of β″ particles does not occur in alloy B3 as much as in alloys B1 and B2. This aspect of the DSC curves is also likely to be closely related to the experimental results shown in the previous works on two-step ageing.

To consider the stability of the metastable/stable phases, the DSC measurements were carried out for the specimens isothermally preaged at 210, 240, 300 and 420 °C. The measurements enable us to link the experimental results due to isothermal ageing with the DSC curve which is normally obtained at constant heating rate.

Fig. 4 shows the changes of the DSC curves for the alloy B2 preaged at 210, 240, 300 and 400 °C. The exothermic peaks K disappear in all DSC measurements for preaged specimens. Furthermore, in the DSC curves obtained for the specimens aged at 210 °C (Fig. 4a), the most significant change appears at peak P. That is, the preliminary annealing at 210 °C decreases the peak height of P with ageing time, whereas other exothermic peaks are merely altered. On the other hand, Fig. 4b shows that the peak Q changes as

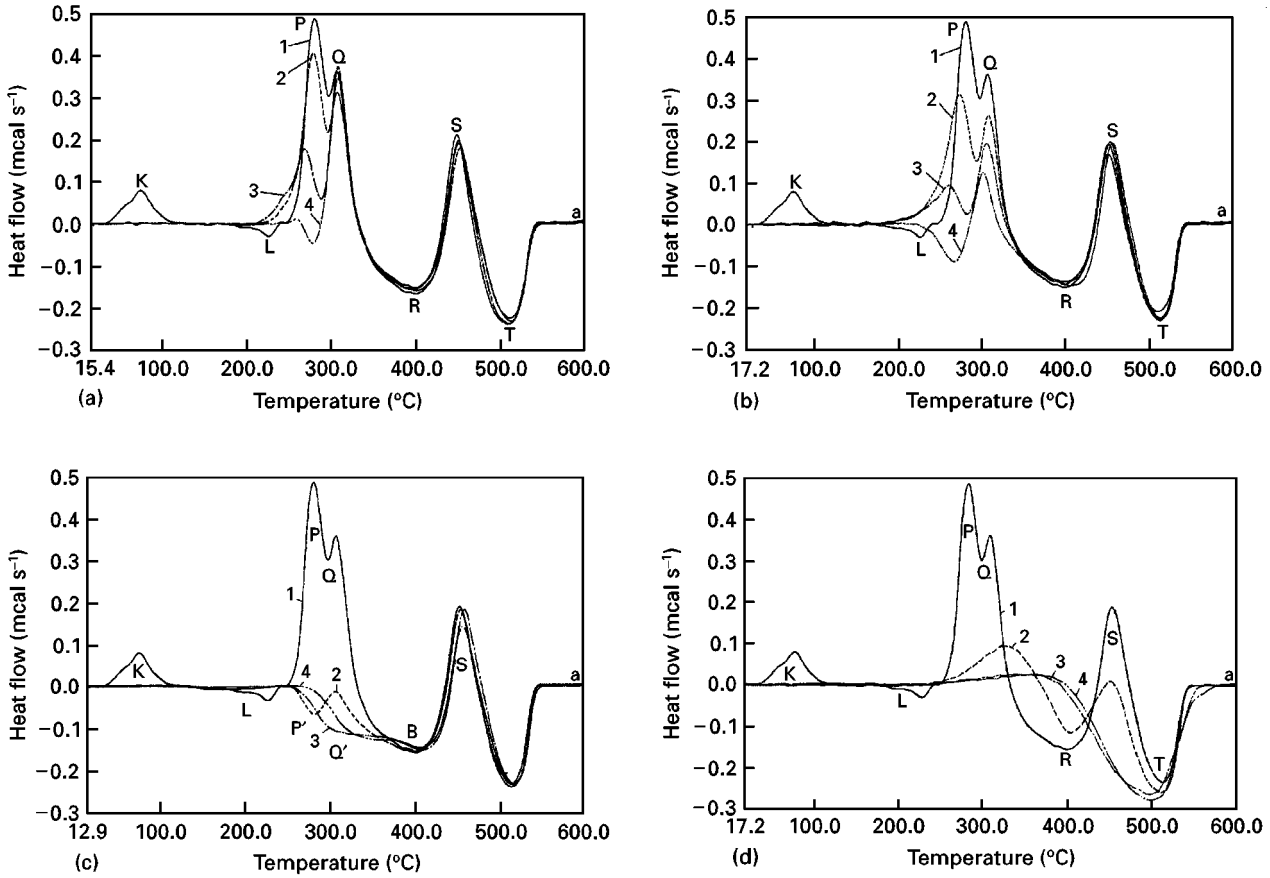


*Figure 4* DSC curves of Al–Mg–Si B2 alloy preaged at (a) 210 °C, (b) 240 °C, (c) 300 °C and (d) 420 °C. (a) (1) As-quenched, (2) 20 min, (3) 100 min, (4) 200 min. (b) (1) As-quenched, (2) 20 min, (3) 50 min, (4) 100 min. (c, d) (1) As-quenched, (2) 10 min, (3) 100 min, (4) 1000 min.

well as peak P under isothermal ageing at 240 °C. The DSC curves of isothermal ageing at 300 °C (Fig. 4c) show that the reduction also occurs at peaks P and Q but not at peak S. In the DSC curves for the specimens preaged at 420 °C, the exothermic peaks S at the highest temperature are also changed in shape. The stable phase at peak S was formed during annealing at 420 °C. The systematic DSC measurements clearly show that the decomposition of phases corresponding to peaks P occurs during isothermal annealing below 210 °C up to 200 min. On the other hand, the decomposition of the phase corresponding to peak Q proceeds during isothermal annealing at 240 and 300 °C.

Fig. 5a shows DSC curves of the solution-treated alloys B2, S3 and M3. The magnitude of peak P is largest for the alloy S3 and smallest for the alloy B2. The order of the peak height in the DSC measurements corresponds to the peak height of the Vickers hardness curves shown in Fig. 2. The peak position in the Vickers hardness can be related to the precipitation hardening due to the precipitation of the β″ phase. Fig. 5b shows the DSC curves obtained for specimens of alloys B2, S3 and M3 preaged at 210 °C for 100 min. The exothermic peak P in alloy S3 is much reduced compared with the curve for the alloy B2. The reduction is attributed to the reaction of β″ formation in the alloy with excess silicon, because the microstructure obtained by TEM observation mainly shows fine needle-like precipitates under the preageing. The reduction of peak P is also observed in the DSC curve for alloy M3 with excess magnesium. This might be caused by the reaction of β″ formation with the addition possibility of a reduction in the quantity of β″ precipitates. Under the preageing, both at 210 and 240 °C, there is no significant exothermic peak between peaks P and Q, although a very small peak before peak P may be considered. As far as the present DSC curves are concerned, it seems that no metastable reaction, which is due to the formation of other metastable phases except β″ and β′, is realized.

As far as the composition of the β″ phase is concerned, it does not seem possible to accept straightforwardly that the quantity of β″ phase increases both in alloys S3 and in M3, if the phase is composed of a stringent composition ratio such as $Mg_2Si$. Taking the Vickers hardness curves and the DSC curves into account, we may draw a possible interpretation such that the composition of the β″ phase is not strictly due to the ternary alloy system, and the composition of the β″ phase is shifted towards the silicon-rich side from $Mg_2Si$, that is, $Mg_{2-}Si$ or $Mg_2Si_+$, which means a portion of the silicon sites in the precipitate can be replaced to some extent by aluminium atoms or vacancies if silicon is deficient. The present idea provides a consistent interpretation of the sensitivity of a silicon addition higher than that of the magnesium addition in the Vickers hardness curves, and the magnitudes of peak P in the DSC measurements obtained in this work, although further investigation of the composition of the β″ phase is crucial to examine whether or not the interpretation is acceptable.

## 3.3. Microstructure of Al–Mg–Si alloys

The present interpretation of the precipitation behaviour of Al–Mg–Si alloys, which is based on macroscopic data such as the Vickers microhardness and DSC, has been examined by microscopic TEM observations. Fig. 6 shows the bright-field TEM images of the microstructures in the alloys B1–B3 under isothermal annealing at 210 °C. The micrographs show that the precipitates corresponding to the peak conditions of B1 and B2 are similar to each other. At these conditions, needle-like precipitates accompanying high strain contrast are mainly observed, and other precipitates, such as thick rods, do not appear. The total quantity of precipitates in alloy B1 is more than that in alloy B2. In the microstructure in alloy B3, on the other hand, neither the shape of the precipitate nor the quantity are similar to alloys B1 and B2, even for short annealing periods. The difference in the microstructure between B1, B2 and B3 is consistent with the results obtained by the Vickers microhardness test and the DSC measurement.

Fig. 7 shows the microstructures of alloys B2, S3 and M3. At the peak position of the $H_v$ curves, the microstructures of alloys B2, S3 and M3 show that most of the precipitates are similarly needle-like. This means that the precipitates which play a major role in increasing $H_v$ hardness are the needle-like precipitates which we relate to peak P in the DSC curves, referred

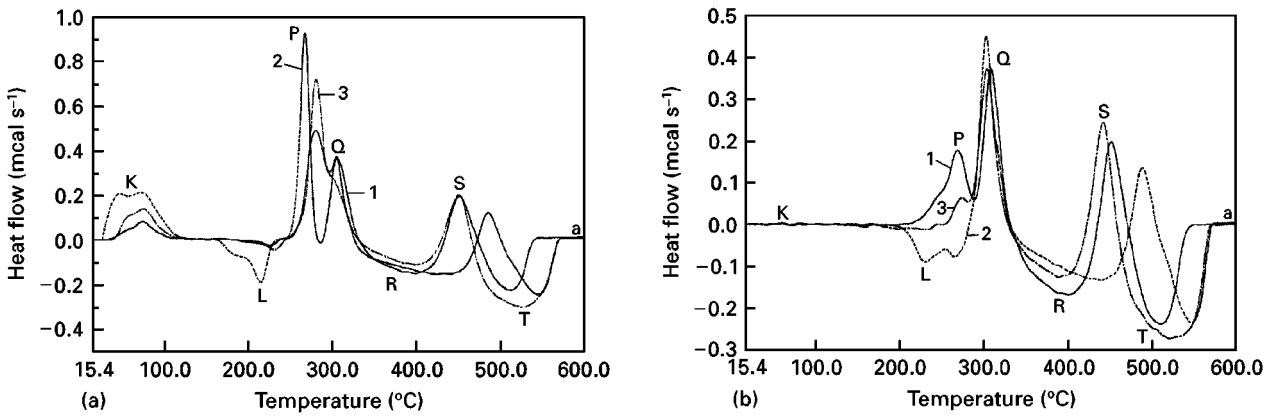


*Figure 5* DSC curves of Al–Mg–Si (1) B2, (2) S3 and (3) M3 alloys, (a) solution-treated, and (b) preaged.

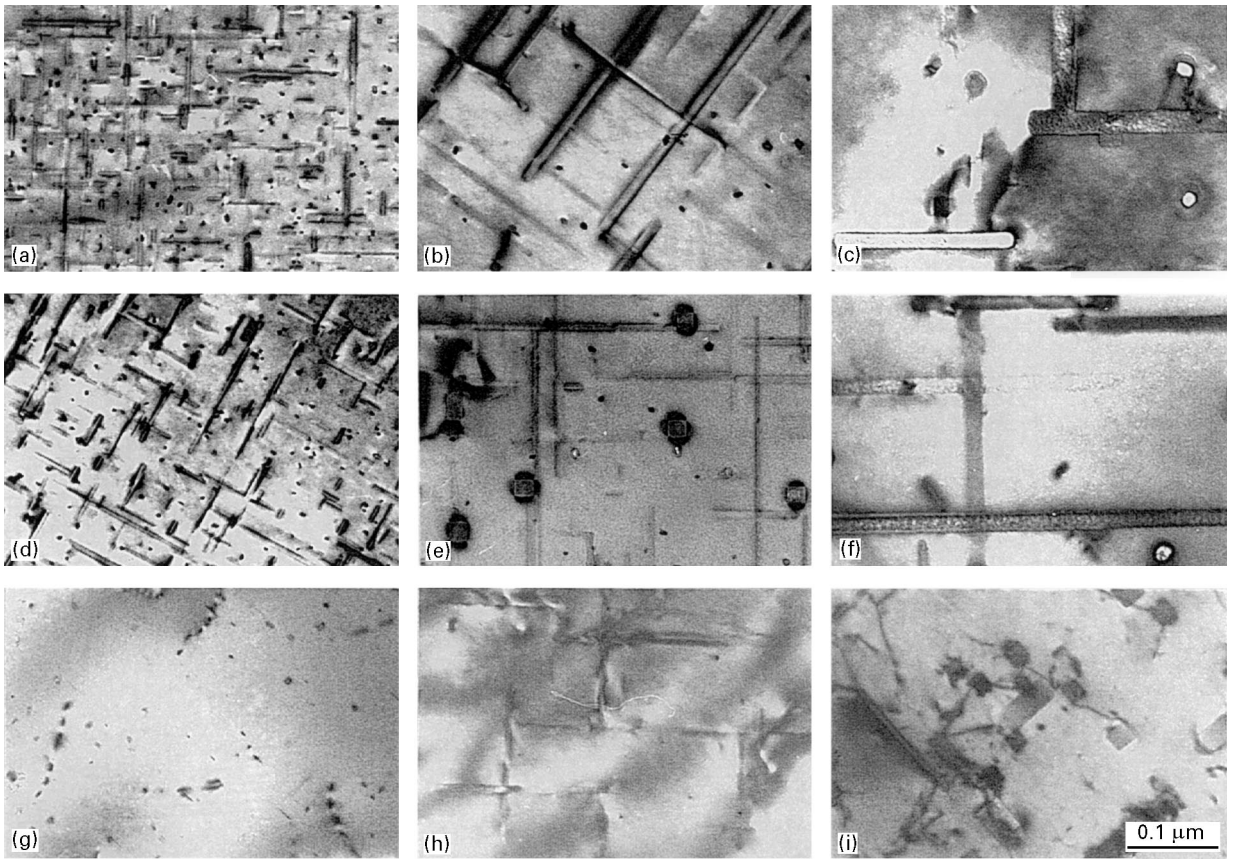


*Figure 6* Microstructures of Al–Mg–Si B1–B3 alloys isothermally aged at 210 °C. (a–c) B1, (d–f) B2, (g–i) B3, for (a, d, g) 100 min, (b, e, h) 1000 min and (c, f, i) 10 000 min.

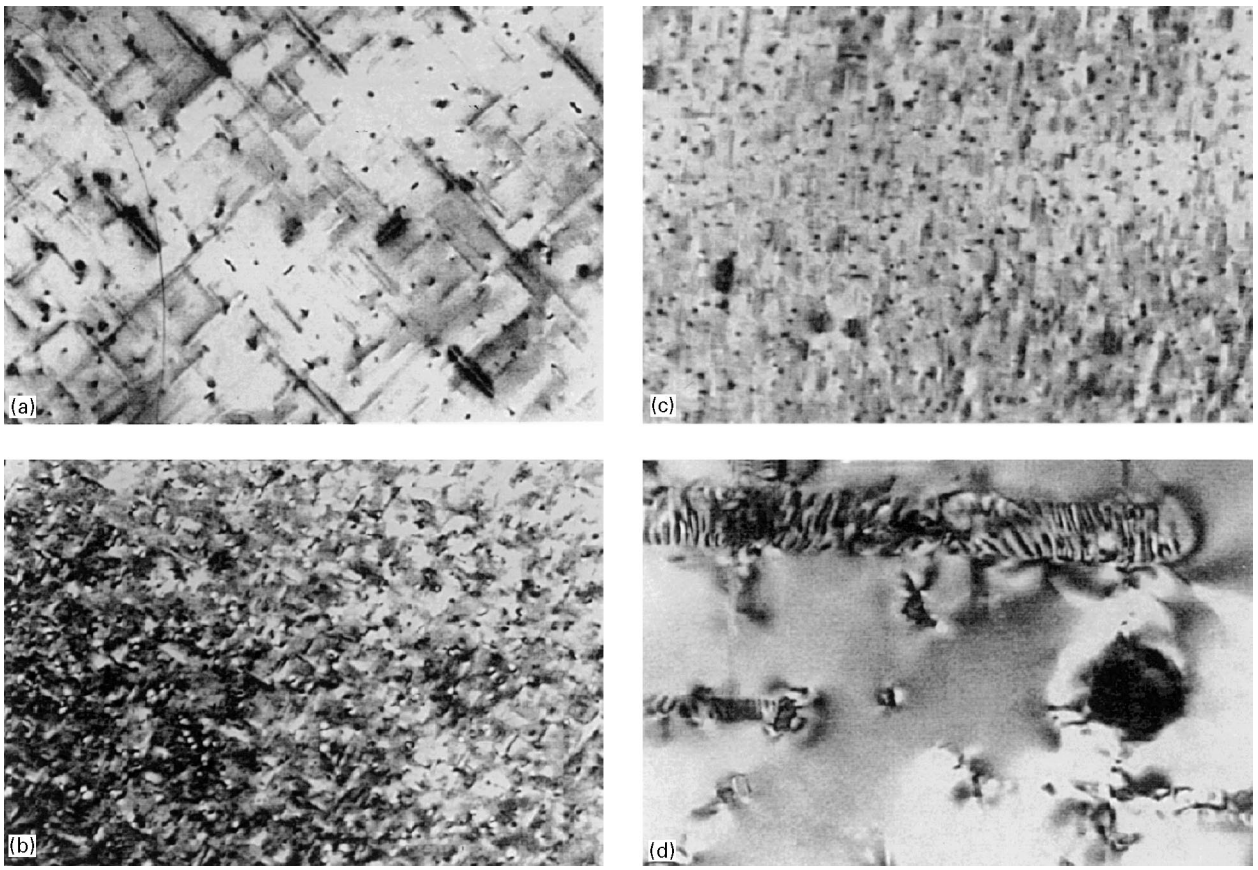


*Figure 7* Microstructures of Al–Mg–Si (a) B2, (b) M3 and (c, d) S3 alloys, (a–c) at 210 °C, 100 min, (d) 210 °C, 10 000 min.

to as β″ phase. Because the peak of the Vickers hardness curve at 240 °C is much lower than the peak at 210 °C, the contribution of the β′ phase is much less than that of the β″ phase. The present TEM observations confirm that the precipitates mainly contribute to the peaks of the Vickers hardness curves in both the balanced alloy and Si/Mg excess alloys.

## 4. Conclusion

The present investigation has shown the relation of the ageing sequences of solute clusters/precipitates in Al–Mg–Si alloys with the DSC thermograms and the microstructures, by systematic DSC measurement, TEM observations and Vickers microhardness tests. DSC measurements clearly showed the different behaviour of the precipitation between the alloys comprising Al–$Mg_2Si$ with more than 0.8–0.9 at % and the alloy with a lower solute composition. Needle-like β″ precipitates play the major role in the age-hardening. The formation of the metastable β″ phase is independent of that of the β′ phase during isothermal heat treatment. No significant exothermic peak was detected, which suggested some phases proposed by Matsuda *et al.* [2] and Edwards *et al.* [3]. The results obtained in this work suggest the composition of the β″ phase is shifted from $Mg_2Si$ towards a silicon-rich composition, and the lattice site of silicon in the precipitate is replaced by aluminium atoms or vacancies if the silicon ratio is deficient.

## References


1. G. THOMAS, *J. Inst. Metals.* **90** (1961–2) 57.
2. M. H. JACOBS, *Philos. Mag.* **26** (1972) 1.
3. P. BARCZY and F. TRANTE, *Scand. J. Metals* **4** (1975) 284.
4. I. DUTTA and S. M. ALLEN, *J. Mater. Sci. Lett.* **10** (1991) 323.
5. J. P. LYNCH, L. M. BROWN and M. H. JACOBS, *Acta Metall* **30** (1982) 1389.
6. K. MATSUDA, Y. UETANI, H. ANADA, S. TADA and S. IKENO, Proceedings of 3rd International Conference on Aluminium Alloys (ed.) L. Anberg *et al.*, (Tronheim, 1992) p. 272.
7. G. A. EDWARDS, G. L. DUNLOP and M. J. COUPER, Proceedings of 4th International Conference on Aluminium Alloys (ed.) T. H. Saunders *et al.*, (Atlanta, 1994) p. 620.
8. R. KAWACHI, *Keikinzoku* **14** (1955) 47.
9. D. W. PASHLEY, J. W. RHODES and A. SENDOREK, *J. Inst. Metals* **94** (1966) 41.
10. Y. BABA and A. TAKASHIMA, *Keikinzoku* **19** (1969) 90.



*Received 7 February 1997*
*and accepted 27 January 1998*